Genetic and dietary modulators of the inflammatory response in the gastro-intestinal tract of the BXD mouse genetic reference population

Xiaoxu Li[1], Jean-David Morel[1], Giorgia Benegiamo[1], Johanne Poisson[1], Alexis Bachmann[1], Alexis Rapin[1], Evan Williams[3], Alessia Perino[2], Kristina Schoonjans[2], Maroun Bou Sleiman[1,*], Johan Auwerx[1,*]

[1]Laboratory of Integrative Systems Physiology, Institute of Bioengineering, École Polytechnique Fédérale de Lausanne, 1015 Lausanne, Switzerland.

[2]Laboratory of Metabolic Signaling, Institute of Bioengineering, École Polytechnique Fédérale de Lausanne, 1015 Lausanne, Switzerland.

[3]Luxembourg Centre for Systems Biomedicine, University of Luxembourg, Luxembourg, Luxembourg.

*e-mail for correspondence: maroun.bousleiman@epfl.ch (MBS) or admin.auwerx@epfl.ch (JA)

Abstract

Inflammatory gut disorders, including inflammatory bowel disease (IBD), can be impacted by dietary, environmental and genetic factors. While the incidence of IBD is increasing worldwide, we still lack a complete understanding of the gene-by-environment interactions underlying inflammation and IBD. Here, we profiled the colon transcriptome of 52 BXD mouse strains fed with a chow or high-fat diet (HFD) and identified a subset of BXD strains that exhibit an IBD-like transcriptome signature on HFD, indicating that an interplay of genetics and diet can significantly affect intestinal inflammation. Using gene co-expression analyses, we identified modules that are enriched for IBD-dysregulated genes and found that these IBD-related modules share *cis*-regulatory elements that are responsive to the STAT2, SMAD3, and REL transcription factors. We used module quantitative trait locus (ModQTL) analyses to identify genetic loci associated with the expression of these modules. Through a prioritization scheme involving systems genetics in the mouse and integration with external human datasets, we identified *Muc4* and *Epha6* as the top candidates mediating differences in HFD-driven intestinal inflammation. This work provides insights into the contribution of genetics and diet to IBD risk and identifies two candidate genes, *MUC4* and *EPHA6*, that may mediate IBD susceptibility in humans.

Keywords: BXD genetic reference population (GRP), System genetics, Inflammatory bowel disease (IBD), High-fat diet (HFD), Chow diet (CD), Weighted gene correlation network analysis (WGCNA), Transcription factors (TFs), Module quantitative trait locus (ModQTL) mapping

43 **Introduction**

44 A long-term lipid-rich diet is associated with multiple metabolic disorders, such as obesity
45 (Hasegawa *et al.*, 2020), cardiovascular disease (Lutsey, Steffen and Stevens, 2008; Maurya *et*
46 *al.*, 2023), and systemic low-grade inflammation (Duan *et al.*, 2018; Christ, Lauterbach and
47 Latz, 2019). The gastro-intestinal tract is the primary site of adaptation to dietary challenge,
48 due to its roles in nutrient absorption, immunity and metabolism (Enriquez *et al.*, 2022).
49 Dietary challenges or other environmental or genetic factors can lead to prolonged
50 inflammation and eventually damage the gastro-intestinal tract (Huang *et al.*, 2017; Enriquez
51 *et al.*, 2022). IBD encompasses several chronic inflammatory gut disorders, including
52 ulcerative colitis (UC) and Crohn's disease (Chang, 2020; Adolph *et al.*, 2022). Patients with
53 IBD, have a higher risk of developing colorectal cancer (CRC), one of the most lethal cancers
54 (Kim and Chang, 2014; Shah and Itzkowitz, 2022). The incidence of IBD has increased
55 worldwide (Alatab *et al.*, 2020; Freeman *et al.*, 2021) during the last decade, in part due to
56 increased consumption of lipid-rich diets (Maconi *et al.*, 2010; Hou, Abraham and El-Serag,
57 2011). Furthermore, mouse studies show that HFD leads to more inflammation in the dextran
58 sulfate sodium (DSS)-induced UC models compared to normal diet (Zhao *et al.*, 2020).
59 However, the response to HFD is variable across individuals (Zeevi *et al.*, 2015) and the
60 association between the lipid-rich diet and the risk of IBD in clinical studies is inconclusive
61 (Kreuter *et al.*, 2019), possibly due to genetic factors underlying inter-individual variability in
62 gut inflammation and dysbiosis (Baumgart and Sandborn, 2012). More than 200 risk genes
63 associated with IBD were identified through human genome-wide association studies (GWAS)
64 (Huang *et al.*, 2017), which have implicated epithelial function, microbe sensing and restriction,
65 and adaptive immune response as drivers (Graham and Xavier, 2020; Kong *et al.*, 2023).
66 However, there is still no effective treatment for IBD. Current therapies, such as anti-tumor
67 necrosis factor alpha (TNF-α) antibodies (Rutgeerts *et al.*, 2005) and integrin α4β7 antibodies,

68 blocking leukocyte migration (Feagan *et al.*, 2013), can temporarily alleviate inflammation in
69 a subset of patients (Rutgeerts *et al.*, 2005; Feagan *et al.*, 2013) but cause adverse effects
70 (Harbord *et al.*, 2017) and fail to prevent relapses (Doherty *et al.*, 2018). Therefore, it is
71 important to understand the gene-by-environment (GxE) interactions underpinning pre-clinical
72 gut inflammation that eventually evolves into IBD, to aid in designing novel preventive and
73 therapeutic strategies for intestinal inflammatory disorders.

74 Heterogeneity in clinical presentations as well as diversity in diet and lifestyle among human
75 IBD patients render human genetic studies challenging (Molodecky *et al.*, 2011). Experiments
76 in laboratory mice allow to control several environmental factors, such as temperature and diet,
77 when exploring the genetic modulators of IBD and also enable the collection of several relevant
78 tissues to help elucidate tissue-specific mechanisms (Nadeau and Auwerx, 2019; Li and
79 Auwerx, 2020). In addition, to mirror the heterogeneity of human populations, genetically
80 diverse populations, such as mouse genetic reference populations (GRPs), can be used in a
81 systems genetics paradigm (Nadeau and Auwerx, 2019; Li and Auwerx, 2020). This not only
82 allows the mapping of clinically relevant traits in controlled environments but also the
83 characterization of intermediate molecular phenotypes from tissues that cannot easily be
84 obtained in humans (Williams *et al.*, 2016; Li and Auwerx, 2020). For example, studies on the
85 molecular basis of non-alcoholic fatty liver disease in the Collaborative Cross founder strains
86 illustrated the importance of the genetic background in determining susceptibility to steatosis,
87 hepatic inflammation and fibrosis (Benegiamo *et al.*, 2023). Moreover, the BXD GRP was used
88 to identify genetic variants associated with metabolic phenotype variation, such as bile acid
89 homeostasis (Li *et al.*, 2022), lipid metabolism in plasma (Jha, McDevitt, Halilbasic, *et al.*,
90 2018) and liver (Jha, McDevitt, Gupta, *et al.*, 2018) as well as mitochondrial dysregulation
91 (Williams *et al.*, 2016), using GWAS or quantitative trait locus (QTL) mapping (Wu *et al.*,

92 2014; Williams *et al.*, 2016). Thus, large mouse GRPs are useful tools for identifying the tissue-
93 specific mechanisms of complex diseases.

94 In order to decipher the genetic and environmental contributions to the development of
95 intestinal inflammation, we measured the colon transcriptome of 52 BXD strains fed with CD
96 or HFD (Williams *et al.*, 2016). HFD feeding from 8 to 29 weeks of age induced an IBD-like
97 transcriptomic signature in colons of some, but not all, BXD strains, uncovering a subset of
98 BXD strains that could be susceptible to HFD-induced IBD-like state. Gene co-expression
99 analysis revealed two IBD-related modules in the colons of HFD-fed mice, one of which is
100 likely under the control of a ModQTL. Through a systems genetics prioritization of genes under
101 this ModQTL, we identified candidate IBD-related genes that we validated using GWAS in the
102 UK Biobank (UKBB) for human IBD.
103

104 **Results**

105 *HFD feeding leads to highly variable transcriptomic adaptations in the colon of BXD strains*

106 For this study, we used an extensively characterized BXD mouse panel of 52 BXD strains fed
107 with a chow diet (CD) or high-fat diet (HFD) from 8 to 29 weeks of age (Williams *et al.*, 2016;
108 Jha, McDevitt, Gupta, *et al.*, 2018; Jha, McDevitt, Halilbasic, *et al.*, 2018), in which we mapped
109 genetic determinants of metabolic traits in the liver (Williams *et al.*, 2016; Jha, McDevitt,
110 Gupta, *et al.*, 2018) and plasma (Jha, McDevitt, Halilbasic, *et al.*, 2018). These mice underwent
111 metabolic phenotyping, with many metabolic traits being altered by HFD (**Figure 1A**), and
112 multiple organs were harvested and flash-frozen for future use (Williams *et al.*, 2016). Here,
113 we focused on proximal colon samples from this population and performed microarray-based
114 transcriptome analysis of this tissue (**Figure 1A**).

115 Principal component analysis (PCA) of all transcriptomes (**Figure 1—figure supplement 1A**)
116 showed that the first principal component (PC1) separated mice by diet, indicative of a global
117 diet effect in the population. Nevertheless, transcriptomes of several strains (such as BXD12,
118 BXD84 and BXD81) on HFD had very similar PC1 values to their CD counterparts (**Figure**
119 **1—figure supplement 1B**), suggesting that they were resistant to dietary changes. Similarly,
120 BXD strains did not cluster completely by diet based on hierarchical clustering analysis
121 indicating that the genetic differences can override the impact of diet on the transcriptome in
122 the colon (**Figure 1—figure supplement 1C**). To obtain a global, strain-independent, view of
123 the HFD effect, we performed a differential expression analysis and identified 115 up- and 295
124 down-regulated differentially expressed genes (DEGs, absolute Log_2(Fold Change) > 0.5 and
125 Benjamini-Hochberg (BH)-adjusted P value < 0.05, **Figure 1B**). Of note, *Cldn4*, one of
126 claudins implicated in intestinal permeability (Ahmad *et al.*, 2017), was significantly down-
127 regulated and serum amyloid A (*Saa1* and *Saa3*), which have been involved in the
128 inflammatory response (Ye and Sun, 2015; Tannock *et al.*, 2018), were up-regulated upon HFD

129 (**Figure 1B**). Furthermore, gene set enrichment analysis (GSEA) showed an upregulation of
130 inflammation, cell proliferation and translation, mitochondrial respiration, and stress response-
131 related pathways upon HFD, while genes involved in the intermediate filament - that contribute
132 to maintaining intestinal barriers (Misiorek *et al.*, 2016; Mun, Hur and Ku, 2022) - were down-
133 regulated (**Figure 1C**). All in all, the transcriptome data are consistent with an HFD-induced
134 downregulation of components of the intestinal barrier, enhanced permeability, induction of
135 the unfolded protein response (UPR) and increased inflammation in BXD colons, much like
136 HFD does in humans (Bischoff *et al.*, 2014). However, as in humans, not every strain exhibited
137 the same response to dietary challenges. GSEA analyses applied individually to the diet effect
138 in each strain showed a high degree of diversity in the inflammatory response (**Figure 1—**
139 **figure supplement 1D**). For example, BXD44, 45 and 55, highlighted in red, were the 3 most
140 susceptible strains to gut inflammation upon HFD, whereas BXD1, 67, and 85, colored in green,
141 showed no significant enrichment in gut inflammation. This diversity in responses provided
142 the basis for a systems genetics investigation of HFD-driven gut inflammation determinants in
143 the BXD.

144 *The transcriptomic response to HFD of a subset of BXD strains resembles DSS-induced*
145 *ulcerative colitis (UC)*

146 IBD is characterized by increasing inflammation in the gastro-intestinal tract (Adolph *et al.*,
147 2022). To investigate the disease relevance of the chronic inflammation seen in BXD colons
148 upon HFD, we extracted the transcriptomic signatures from DSS-induced mouse UC models
149 (Czarnewski *et al.*, 2019) and two IBD human studies (GSE16879 (Arijs *et al.*, 2009) and
150 GSE83687 (Peters *et al.*, 2017), **Materials and Methods**) and used these signatures as custom
151 gene sets in GSEA on the global HFD effect. DSS is widely used to induce UC in mouse
152 models and disease severity increases over time (Czarnewski *et al.*, 2019). GSEA analyses
153 showed that DSS-induced genes from days 4 (early inflammatory phase), 6 and 7 (acute

154 inflammatory phase) were significantly enriched in genes upregulated by HFD, especially the
155 dysregulated genes in the later stage of DSS-induced UC (**Figure 1D, bottom panel**). Similarly,
156 genes involved in human IBD (UC and Crohn's disease (CDs)) were also enriched in those
157 same genes (**Figure 1D, top panel**). The same trend was observed for downregulated genes in
158 mouse and human IBD, which were negatively enriched (**Figure 1D**), illustrating that HFD
159 induced an IBD-like transcriptomic signature in BXD colons.

160 While the average response across all BXDs shared features of mouse and human IBD, we
161 assessed the strain-specificity of this response by measuring each strain's response to IBD
162 using GSEA (**Figure 2A**). Hierarchical clustering of the normalized enrichment scores (NES)
163 in mouse IBD datasets classified the BXDs into three groups: susceptible strains highlighted
164 in red (19 strains), intermediate strains represented in blue (11 strains), and resistant strains
165 colored in green (17 strains) (**Figure 2A, top panel**). Of note, in line with colon histological
166 lesions comparison of DSS-induced colitis mouse models in the literature (Mähler *et al.*, 1998),
167 the C57BL/6J strain, one of the parental strains of the BXDs, was classified as one of the
168 susceptible strains while the other parental strain DBA/2J belonged to the resistant group
169 (**Figure 2A, top panel**), suggesting that genetic determinants inherited from the parental strains
170 may determine the susceptibility of BXD strains to HFD-induced IBD-like inflammation in the
171 colons.

172 To establish the functional relevance of this transcriptome-based classification on systemic
173 inflammation, we compared plasma cytokine levels of these three groups under HFD (Williams
174 *et al.*, 2016). Interestingly, the susceptible group have significantly lower levels of the anti-
175 inflammatory cytokine - Interleukin (IL)-10 (**Figure 2B,** two-tailed t-test $p < 0.01$) and
176 increased the proinflammatory cytokine - IL-15 (**Figure 2C,** two-tailed t-test $p < 0.0001$)
177 compared to the resistant strains. *IL10* itself has been identified as an IBD-related candidate
178 gene using GWAS in humans (Franke *et al.*, 2008) and IL-10-deficient mice are also well-

179 known mouse model for IBD research (Keubler *et al.*, 2015). IL-15 is another important
180 cytokine involved in intestinal inflammation and is elevated in the human guts with IBD (Liu
181 *et al.*, 2000). IL-15 knock-out mice are also reported to have less severe symptoms, such as
182 weight loss and histological scores, following DSS administration (Yoshihara *et al.*, 2006). In
183 summary, susceptibility to HFD-induced IBD-like inflammation in the colon, as assessed by
184 changes in levels of genes associated with IBD, correlates with markers of the general
185 inflammatory status of mice.

186 *Identifying IBD-related gene modules in BXD colons*

187 Since different BXD strains seem to exhibit different susceptibility to IBD, we set out to
188 explore gene expression signatures underlying these differences. For that, we used Weighted
189 Gene Co-expression Analysis (WGCNA) to construct CD- and HFD-specific gene co-
190 expression networks to identify modules of co-expressed genes (**Figure 3A, Appendix 1 -**
191 **Table 1**). Disease-associated modules were then defined as modules under HFD are
192 significantly enriched in mouse DSS-induced UC signatures by an over-representation analysis
193 (ORA, BH-adjusted P value < 0.05 and number of enriched genes > 5, **Figure 3A**). The HFD
194 co-expression network consisted of 39 modules ranging in size from 34 to 1,853 genes and
195 containing a total of 14,723 genes (**Appendix 1 - Table 1**). We visualized this network using
196 Uniform Manifold Approximation and Projection (UMAP) (**Figure 3B**), reflecting that the
197 majority modules were closely connected in the co-expression network.

198 Enrichment analyses indicated that modules HFD_M9, HFD_M16, and HFD_M28 were
199 enriched with genes that are upregulated by DSS-induced colitis, while HFD_M15, HFD_M24,
200 and HFD_M26 were significantly enriched with downregulated genes **(Figure 3C).** Of note,
201 more than 20% of genes involved in HFD_M9 and HFD_M28 were part of the dysregulated
202 genes of the acute phase of mouse UC (day6 and day7) (**Figure 3C**). Interestingly, genes

203 perturbed during IBD pathogenesis in humans were also enriched in HFD_M9 and HFD_M28
204 (**Figure 3C**).

205 While IBD-related genes were predominantly found in HFD modules, we also found that two
206 modules, CD_M28 and CD_M32, in CD-fed mouse colons were associated with IBD (**Figure**
207 **3—figure supplement 1A)**. These two-modules significantly overlapped with the IBD-related
208 HFD_M9 and HFD_M28 modules, respectively (BH-adjusted P value < 0.05) (**Figure 3—**
209 **figure supplement 1B)**. Moreover, the molecular signatures underlying human UC and
210 Crohn's disease were also clustered in these two modules (CD_M28 and CD_M32) under CD
211 (**Figure 3—figure supplement 1C**). Collectively, the co-expression and enrichment analyses
212 identify HFD_M9 and HFD_M28 as IBD-related modules on which we focus our subsequent
213 investigation.

214 *Identifying biological roles and transcriptional regulation of the IBD-related modules*

215 To identify the biological function of the IBD-related modules, we performed enrichment
216 analyses using the Hallmark database and the cell-type gene signatures (Kong *et al.*, 2023)
217 (**Materials and Methods**). Genes in HFD_M9 were enriched in KRAS signaling and
218 inflammation-related pathways, while HFD_M28 was enriched in IFN-α/γ responses (BH-
219 adjusted P value < 0.05) (**Figure 4A**). Both modules were enriched in IFN-γ response genes
220 (**Figure 4A**). IFN-γ is an essential cytokine for innate and adaptive intestinal immune responses
221 (Brasseit *et al.*, 2018). It has been reported to play a key role in mouse (Ito *et al.*, 2006) and
222 human (Tilg *et al.*, 2002) IBD pathogenesis, and was identified as a potential therapeutic target
223 to alleviate inflammatory response in IBD (Li *et al.*, 2021). In addition, genes that are
224 dysregulated in immune cells of Crohn's disease patients (Macrophages, B cell and immune
225 cycling cells) were enriched in HFD_M9 (**Figure 4B**). In contrast, genes of HFD_M28 were
226 not only enriched for genes that are dysregulated in immune cells, but also in intestinal
227 epithelial cells of diseased individuals, such as Goblet and stem cells (**Figure 4B**). Overall,

228 HFD_M9 and HFD_M28 are both involved in inflammatory response, while genes involved
229 in HFD_M28 also potentially influence intestinal epithelial barrier.

230 To identify transcriptional drivers of the two IBD-related modules, we performed a
231 transcription factor (TF) enrichment analysis (**Materials and Methods**) and found that ZIC2,
232 SMAD3, REL, FOSL1, and BATF are the top enriched transcription factors for the genes in
233 HFD_M9 (**Figure 4C**), while the expression of genes in module HFD_M28 may be regulated
234 by Interferon regulatory factors (IRFs, IRF1, IRF2, IRF7, and IRF9) and the signal transducer
235 and activator of transcription families (STAT, STAT2) (**Figure 4D**). In fact, most of these TFs
236 have been reported to be involved in gut inflammation. For example, *Smad3* mutant mice were
237 more susceptible to intestinal inflammation (Yang *et al.*, 1999). Moreover, the IFN-STAT axis
238 is essential to initiate the type-I IFN induction that is critical for human immune defense, such
239 as IBD diseases (Stolzer *et al.*, 2021) and primary immunodeficiency diseases (Mogensen,
240 2019) as well as for disease tolerance (Mottis *et al.*, 2022). Collectively, we have identified
241 TFs that likely control the expression of the two IBD-related modules to play an essential role
242 in gut inflammation regulation.

243 *Identifying ModQTLs for IBD-related modules and filtering of candidate genes*

244 To analyze how the genotype impacts the IBD-like inflammatory response associated to HFD,
245 we performed module QTL mapping analysis (ModQTL) for both IBD-related modules
246 (HFD_M9 and HFD_28) (**Figure 5A**). We found a suggestive QTL for HFD_M28 (P value <
247 0.1), on chromosome 16 containing 552 protein-coding genes (**Figure 5A, Appendix 1 - Table**
248 **2**). We annotated these candidate genes based on three criteria (**Figure 5B**): (1) presence of
249 high-impact genetic variants (such as missense and frameshift variants) in BXDs, (2)
250 association with inflammation based on literature mining (**Materials and methods**), (3)
251 presence of *cis*-expression QTLs (eQTLs), that is, whether the expression of the gene is

252 controlled by the QTL. The 27 genes satisfying at least two of the above criteria were
253 considered as candidate genes driving the expression of module HFD_M28 (**Figure 5C**).

254 To further prioritize candidate genes regulating module HFD_M28, we applied GWAS to
255 detect Crohn's disease- and UC-associated genetic variants using whole genome sequence
256 (WGS) dataset in UKBB (**Figure 5C, Materials and Methods**). Interestingly, the genetic
257 variants of two genes under the QTL peak, i.e, *ephrin type A receptor 6* (*EPHA6,* P value =
258 2.3E-06) (**Figure 5C**, **Figure 5—figure supplement 1A**) and *Mucin 4* (*MUC4,* P value = 1.2E-
259 06) (**Figure 5C**, **Figure 5—figure supplement 1B)** were also associated with UC in humans.
260 *EPHA6* belongs to Eph/Ephrin Signaling and this pathway has been associated with gut
261 inflammation (Coulthard *et al.*, 2012) and proposed as a potential target to alleviate the
262 inflammatory response in IBD (Grandi *et al.*, 2019), but the association between *EPHA6* and
263 IBD is not explored yet. The Gene-Module Association Determination (G-MAD) (Li *et al.*,
264 2019) (https://systems-genetics.org/gmad) also revealed that expression of *Epha6* in mouse
265 gastro-intestinal tract correlates with genes involved in inflammation-related pathways, such
266 as IL-6 production and regulation of inflammatory response (**Figure 5D, Appendix 1 - Table**
267 **3**). *MUC4* is a transmembrane mucin (Gao *et al.*, 2021) and highly expressed in gastro-
268 intestinal tract according to the human protein atlas (Uhlén *et al.*, 2015)
269 (https://www.proteinatlas.org/humanproteome/tissue/intestine) (**Figure 5C**). The expression
270 of *MUC4* in the human gastro-intestinal tract correlates with genes that are enriched for CRC
271 and O-linked glycosylation based on G-MAD (Li *et al.*, 2019) (**Figure 5E, Appendix 1 - Table**
272 **3**). O-linked glycans are expressed by the intestinal epithelium to maintain barrier function,
273 especially mucin type O-glycans, and gut disorders can be affected by dysfunction of O-linked
274 glycosylation (Brazil and Parkos, 2022). Moreover, *MUC4* is upregulated in enterocytes and
275 Goblet cells in colons of Crohn's disease patients (**Figure 5F)**. *MUC4* hence is a strong
276 candidate because of its role in maintaining the intestinal epithelium and controlling the gut

277 inflammatory response (McGuckin *et al.*, 2011) and *EPHA6* might be a novel candidate gene
278 to impact gut inflammation. Based on the results of our QTL mapping, human GWAS in
279 UKBB, and existing literature, we hypothesize that *MUC4* and *EPHA6* impact on colon
280 integrity and inflammation and may be important players in gut inflammation or IBD triggered
281 by an unhealthy, lipid-rich diet.
282

283 **Discussion**

284 Dietary, environmental and genetic factors have all been reported to influence intestinal
285 inflammation (Adolph *et al.*, 2022). Indeed, HFD can impair the intestinal epithelial barrier
286 and trigger pre-clinical inflammation in the gastro-intestinal tract, eventually leading to
287 inflammatory disorders of the gut (Enriquez *et al.*, 2022). In addition, genetic factors identified
288 by GWAS can also predispose to IBD. For example, the interleukin-1 and -7 receptors (*IL-1R2*
289 and *IL-7R*) were identified as candidate genes that regulate the immune response in IBD (Khor,
290 Gardet and Xavier, 2011). However, the heterogeneity of diet and other environmental factors
291 in human studies limits our ability to identify GxE interactions and pinpoint the genes and
292 pathways involved in diet-induced gut inflammation. Studies in model organisms such as the
293 mouse, where the environment can be carefully controlled, provide a valuable complement to
294 human genetics studies that by nature are mainly observational (Nadeau and Auwerx, 2019; Li
295 and Auwerx, 2020). Unfortunately, most mouse studies only evaluate mice from a single
296 genetic background, limiting their generalizability and translatability to humans (Nadeau and
297 Auwerx, 2019; Li and Auwerx, 2020). Conversely, GRPs such as the BXDs can mimic at least
298 in part the heterogeneity of human populations and allow us to estimate the effect of GxE
299 interactions on complex diseases (Jha, McDevitt, Gupta, *et al.*, 2018; Li and Auwerx, 2020).

300 Here, we utilized a panel of 52 BXD genetically diverse mouse strains fed with either HFD or
301 CD to explore the genetic and dietary modulators of inflammation seen in the colon
302 transcriptomes using systems genetics approaches. The colon transcriptomic response to HFD
303 in this mouse population recapitulated several of the general features observed in DSS-induced
304 UC mouse models and human IBD patients. In particular, we identified the upregulation of
305 inflammation-related genes and the UPR as well as the downregulation of intercellular
306 adhesion-related genesets as common signatures induced by HFD (Kreuter *et al.*, 2019).
307 Moreover, our dataset not only was informative about the transcript changes of IBD at the

308 population level, but also unveiled extensive strain-specific effects that allowed us to classify
309 strains based on their propensity to develop IBD-like signatures. The fact that these
310 susceptibility groups also differed in anti- and pro-inflammatory plasma cytokine levels (IL-
311 10 and IL-15, respectively) suggests a relation between these tissue-specific transcriptional
312 signatures and systemic low-grade inflammation. Since gene interactions determine cellular
313 processes and the molecular functions of correlated genes are often similar (Nayak *et al.*, 2009),
314 we attempted to elucidate the mechanism underlying the diversity of IBD-like signatures and
315 chronic inflammation in BXD colons using gene co-expression analyses. This led us to identify
316 two IBD-related gene modules (HFD_M9 and HFD_M28).

317 As most differentially expressed genes are likely to be driven by and not be a cause of disease
318 (Porcu *et al.*, 2021), we attempted to understand whether the signatures in the colon are causes
319 or consequences of chronic inflammation. A first step was to characterize possible
320 transcriptional and genetic regulators of IBD-related modules. Enrichment analyses showed
321 that both IBD-associated modules largely consisted of immune response-related genes.
322 Specifically, genes involved in HFD_M9 and HFD_M28 are both differentially expressed in
323 immune cells in inflamed tissues of Crohn's disease patients (Kong *et al.*, 2023). Moreover,
324 the HFD_M28 module was enriched for TF motifs of STAT2 and IRF family, and HFD_M9
325 for SMAD3 and REL, which were illustrated to control the expression of these gut
326 inflammation-related genes, and influence the inflammatory response triggered by HFD in the
327 colon.

328 While we found IBD-related gene modules and the TFs driving their expression, the genetic
329 drivers of the diversity of gut inflammatory responses observed across the BXDs remained
330 elusive. To find candidate genes causing gut inflammation upon HFD, we then performed
331 Module QTL (ModQTL) analysis and allocated a suggestive ModQTL that may be controlling
332 one of IBD-related module (HFD_M28) under HFD. Importantly, through our prioritization

333 scheme for the genes under the ModQTL, we identify two plausible candidates, *Epha6* and
334 *Muc4*, that have high-impact variants in the BXDs, are related to inflammation, and harbor
335 variants in humans that are associated with IBD based on UKBB GWAS result. In fact, *Muc4*
336 knock-out mice have been shown to be more resistant to DSS-induced UC through
337 upregulating the expression of *Muc2* (mucin secretion) and *Muc3* (transmembrane mucin) (Das
338 *et al.*, 2016) . A GWAS study also indicated that mutations in *EPHA6* increase risk for CRC
339 (Guda *et al.*, 2015), but its potential association with IBD is a new finding. Therefore, these
340 results point to important potential roles of *Muc4* and *Epha6* in gut chronic inflammation
341 leading to inflammatory gut disorders.

342 Although studies in the BXD cohort are limited to variants present in the parental strains,
343 C57BL/6J and DBA/2J, our analysis nevertheless shows how genetic diversity in this
344 population allows us to detect the genetic modulators of chronic intestinal inflammation, that
345 are more difficult to identify in widely used IBD mouse models on a single genetic background.
346 In support of the generalizability of our data, the identified candidate genes in our mouse
347 models were also associated to human UC, demonstrating that chronic inflammation induced
348 upon HFD feeding may indeed be a prelude to human UC.

349 In conclusion, our systems genetics investigation of the colon in a controlled GRP,
350 complemented with human GWAS studies, enabled the prioritization of modulators of IBD
351 susceptibility that were generalizable to the human situation and may have clinical value.
352

353 **Materials and methods**

354 *Population handling*

355 Mice were studied as previously described (Williams *et al.*, 2016) and multiple organs were
356 harvested for further analysis. Briefly, in groups of 3-5 animals from the same strain and diet,
357 in isolator cages with individual air filtration (500 cm2, GM500, Tecniplast) and provided
358 water ad libitum. Mice were fed CD ad libitum until 8 weeks of age. From 8 weeks to 29 weeks,
359 half of the cohort was fed ad libitum HFD and the rest continued to be fed a CD (**Figure 1A**).
360 CD composition: 18% kCal fat, 24% kCal protein and 58% kCal of carbohydrates (Teklad
361 Global 18% Protein Rodent Diet 2018 chow diet, Envigo, Indianapolis, USA). HFD
362 composition: 60.3% kCal fat, 18.4% kCal protein and 27.3% kCal of carbohydrates (Teklad
363 Custom Diet TD.06414, Envigo, Indianapolis, USA). All mice were fasted overnight (from
364 6pm to 9am) prior to euthanasia. All procedures were approved by the veterinary office of
365 canton Vaud under animal experimentation license number VD2257. In this work, proximal
366 colons were extracted from the bio-banked samples and we did not use any new animals.

367 *Transcriptome of the proximal colon in BXDs*

368 A ~1 cm portion of the proximal half part of the colon was excised following euthanasia,
369 washed in PBS and immediately stored in liquid nitrogen. Approximately 5 animals of the
370 same strain fed the same diet were pooled at equal mass concentration for further RNA
371 extraction. Total RNA was extracted using Direct-zol (Zymo Research) including the DNase
372 digestion step. 100ng of total RNA was amplified using the Ambion® WT Expression Kit from
373 Life Technologies (part number 4411974) and 5,500ng of cDNA was fragmented and labeled
374 using the Affymetrix WT terminal labeling kit (part number 900671) all following
375 manufacturers protocols. Labeled cDNA was hybridized on an Affymetrix Clariom S Assay
376 microarray platform (GPL23038) in ~16 hours of incubation, then washed and stained using

377 an Affymetrix 450 Fluidics Station according to Affymetrix protocols. Finally, arrays were
378 scanned on Affymetrix GSC3000 7G Scanner. Microarray data preprocessing was performed
379 using apt-probeset-summarize from the Array Power Tool (APT) suite (v2.11.3) with the gc-
380 sst-rma-sketch standard method and resulting expression values were log-transformed.
381 Microarray probes targeting polymorphic regions in the BXD population were ignored in the
382 process. For probesets targeting a same transcript, only the probeset with the highest value was
383 considered.

384 *Differential gene expression analysis*

385 General differences in mRNA expression profiles between diets was assessed using Principal
386 Component Analysis (PCA). Differential expression of individual transcripts between diets
387 was assessed using the limma R Bioconductor package (version 3.48.3) (Ritchie *et al.*, 2015).
388 Briefly, statistical significance was assessed using an empirical Bayes method (eBayes function)
389 with an additive linear model accounting for diet and strain effect and adjusted P values were
390 calculated by the Benjamini-Hochberg (BH) approach. Transcripts showing BH-adjusted P
391 value below 0.05 and absolute Log_2 (Fold Change) above 0.5 were considered significantly
392 associated with the effect of the diet.

393 *Gene set enrichment analysis (GSEA) and Over-representation analysis (ORA)*

394 Gene sets used in GSEA and ORA consisted of two parts: (1) the gene sets from the GO, KEGG,
395 Hallmark, and Reactome databases were retrieved through the msigdbr R package (version
396 7.2.1) (Liberzon *et al.*, 2011). (2) the gene signatures of mouse and human IBD were used as
397 custom gene sets (**Table 1**).

398 GSEA was performed using clusterProfiler R package (version 3.10.1) (Yu *et al.*, 2012) based
399 on the log_2(Fold Change) ranking using parameters (*nPerm* = 100000, *minGSSize* = 30,

400 *maxGSSize* = 5000, *pvalueCutoff* = 1). The gene sets with absolute NES higher than 1 and BH-
401 adjusted P value lower than 0.05 were identified as the significantly enriched gene sets.

402 ORA analysis was also performed using clusterProfiler R package (version 3.10.1) (Yu *et al.*,
403 2012) using parameters (minGSSize = 30, maxGSSize = 800). The gene sets with adjusted P
404 value calculated by BH lower than 0.05 were identified as the significantly enriched gene sets.

405 *Weighted gene correlation network analysis (WGCNA)*

406 We used *WGCNA* R package (v1.51) (Langfelder and Horvath, 2008) to construct co-
407 expression networks under CD and HFD, respectively. Firstly, the correlations between all
408 pairs of gene across all BXDs fed with CD or HFD were calculated by Pearson correlation.
409 Then, a best soft-thresholding power of 4 and 3 was chosen using pickSoftThreshold function
410 with parameters (*networkType* = "signed hybrid", *blockSize* = 25000, *corFnc* = "bicor") for CD
411 and HFD datasets in BXD colons separately. According to the calculated correlation
412 coefficients, a network was constructed using parameters (*networkType* = "signed hybrid",
413 *minModuleSize* = 30, *reassignThreshold* = 1e-6, *mergeCutHeight* = 0.15, *maxBlockSize* =
414 25000). The constructed co-expression gene modules were assigned color names and the
415 module eigengenes were also identified for further analyses. To detect the preserved CD-
416 modules in the co-expression modules under HFD, we defined gene modules under CD as
417 custom genesets and performed ORA on each HFD-modules.

418 *Transcription factor (TF) enrichment analysis*

419 We first constructed a lognormal background distribution using the sequences of + 5kb region
420 around the transcription starting site (TSS) of all genes and then downloaded the mouse
421 HOCOMOCO-v10 (Kulakovskiy *et al.*, 2018) motifs from R package motifDB to perform TF
422 enrichment analyses using R package *PWMenrich*. The significantly enriched motifs (P value
423 < 0.001) were selected and then ranked based on the percentage of enriched promoters.

424 *Module Quantitative Trait Locus (ModQTL) mapping in the BXDs*

425 We first downloaded genotype information of each BXD mice from GeneNetwork
426 (https://gn1.genenetwork.org/webqtl/main.py?FormID=sharinginfo&GN_AccessionId=600)
427 and generated the kinship matrix of BXD mice using the leave-one-chromosome-out (LOCO)
428 method. We then used the eigengenes of each module as phenotype input to perform Module
429 QTL (ModQTL) with the R package *qtl2* (version 0.28) (Broman *et al.*, 2019) and the threshold
430 of each QTL mapping analysis was obtained from a permutation test with 10,000 repeats. The
431 peaks of QTL were calculated by *find_peaks* function with parameter: *prob=0.95.*

432 The same methods were also applied to gene expression QTL mapping (eQTL) and the
433 significance threshold of each gene was obtained from a permutation test with 1,000 repeats.
434 The significant peaks overlapped with the location of their corresponding gene were identified
435 as *cis*-eQTL.

436 *Literature mining*

437 To explore the inflammation related genes, we first used candidate gene names and keywords
438 ("IBD", "inflammatory bowel disease", "Ulcerative colitis", "Inflammation", "Inflammatory",
439 "Crohn's disease") to search the title or abstract of associated literature using R package
440 easyPubMed (version 2.13). Then, the genes involved in inflammation were confirmed by
441 manual curation.

442 *Genome-wide association study (GWAS) in UKBB*

443 The phenotype data of inflamed Ulcerative colitis (Data-Field 131629, n = 6,459) and Crohn's
444 disease (Data-Field 131627, n = 3,358) were firstly downloaded from UKBB (Bycroft *et al.*,
445 2018). 200,030 individuals with whole genome sequencing (WGS) (Halldorsson *et al.*, 2022)
446 in UK Biobank were selected and then the population of European descent (including with
447 1,173 patients with Crohn's disease and 2,295 patients with UC) was extracted for further

448 GWAS analyses. Control individuals (n = 143,194) were included based on the following
449 criteria: (1) Individuals without non- inflamed colitis (Data-Field 131631), Crohn's disease,
450 and UC. (2) Individuals not taking any IBD-related medicine (**Appendix 1 - Table 4**).

451 WGS data provided by UK Biobank and used for GWAS were processed starting from pVCF
452 files. We used REGENIE step1 to estimate population structure and then REGENIE step2 were
453 applied to test associations between phenotypes and genetic variants and also included the
454 following covariates in our model: the first 10 genetic principal components, age, sex, age:sex
455 interaction, Body Mass Index (BMI), and smoking status. All data preparation and GWAS
456 steps were run on DNAnexus.

457

Acknowledgments

We thank the Schoonjans' and Auwerx's lab members for technical assistance and discussions and Giacomo von Alvensleben for providing the GWAS analysis pipeline in human UKBB. The work in the JA laboratory was supported by grants from the Ecole Polytechnique Fédérale de Lausanne (EPFL), the European Research Council (ERC-AdG-787702), the Swiss National Science Foundation (SNSF 31003A_179435) and the Global Research Laboratory (GRL) National Research Foundation of Korea (NRF 2017K1A1A2013124). XL was supported by the China Scholarship Council (201906050019).

Author contributions

The study was conceived by XL, MBS and JA. EW, MBS and AB performed laboratory experiments. Data analyses were carried out by XL, AB, AR and JP. XL and JA wrote the original manuscript. XL, MBS, JDM, GB, AP, KS and JA reviewed and edited the manuscript with contributions from all co-authors.

Competing interests

Authors declare no conflict of interest related to the work reported.

Data availability

The data that support the findings are available upon request to the corresponding authors (MBS and JA). The microarray data are available under the GEO numbers GSE225791. To review this dataset, please use this link: https://www.ncbi.nlm.nih.gov/geo/query/acc.cgi?acc=GSE225791 and the review token is

exwtuucwpdqlzsr. Methods, materials and external resources are included in the **Materials and Methods**.

483 **References**

484 Adolph, T.E. *et al.* (2022) 'The metabolic nature of inflammatory bowel diseases', *Nature*
485 *Reviews Gastroenterology & Hepatology*, 19(12), pp. 753–767. Available at:
486 https://doi.org/10.1038/s41575-022-00658-y.

487 Ahmad, R. *et al.* (2017) 'Obesity-induces Organ and Tissue Specific Tight Junction
488 Restructuring and Barrier Deregulation by Claudin Switching', *Scientific Reports*, 7(1), p. 5125.
489 Available at: https://doi.org/10.1038/s41598-017-04989-8.

490 Alatab, S. *et al.* (2020) 'The global, regional, and national burden of inflammatory bowel
491 disease in 195 countries and territories, 1990–2017: a systematic analysis for the Global Burden
492 of Disease Study 2017', *The Lancet Gastroenterology & Hepatology*, 5(1), pp. 17–30.
493 Available at: https://doi.org/10.1016/S2468-1253(19)30333-4.

494 Arijs, I. *et al.* (2009) 'Mucosal Gene Expression of Antimicrobial Peptides in Inflammatory
495 Bowel Disease Before and After First Infliximab Treatment', *PLOS ONE*, 4(11), p. e7984.
496 Available at: https://doi.org/10.1371/journal.pone.0007984.

497 Baumgart, D.C. and Sandborn, W.J. (2012) 'Crohn's disease', *The Lancet*, 380(9853), pp.
498 1590–1605. Available at: https://doi.org/10.1016/S0140-6736(12)60026-9.

499 Benegiamo, G. *et al.* (2023) 'The genetic background shapes the susceptibility to mitochondrial
500 dysfunction and NASH progression', *Journal of Experimental Medicine*, 220(4), p. e20221738.
501 Available at: https://doi.org/10.1084/jem.20221738.

502 Bischoff, S.C. *et al.* (2014) 'Intestinal permeability – a new target for disease prevention and
503 therapy', *BMC Gastroenterology*, 14(1), p. 189. Available at: https://doi.org/10.1186/s12876-
504 014-0189-7.

505 Brasseit, J. *et al.* (2018) 'Divergent Roles of Interferon-γ and Innate Lymphoid Cells in Innate
506 and Adaptive Immune Cell-Mediated Intestinal Inflammation', *Frontiers in Immunology*, 9.
507 Available at: https://www.frontiersin.org/articles/10.3389/fimmu.2018.00023 (Accessed: 24
508 February 2023).

509 Brazil, J.C. and Parkos, C.A. (2022) 'Finding the sweet spot: glycosylation mediated regulation
510 of intestinal inflammation', *Mucosal Immunology*, 15(2), pp. 211–222. Available at:
511 https://doi.org/10.1038/s41385-021-00466-8.

512 Broman, K.W. *et al.* (2019) 'R/qtl2: Software for Mapping Quantitative Trait Loci with High-
513 Dimensional Data and Multiparent Populations', *Genetics*, 211(2), pp. 495–502. Available at:
514 https://doi.org/10.1534/genetics.118.301595.

515 Bycroft, C. *et al.* (2018) 'The UK Biobank resource with deep phenotyping and genomic data',
516 *Nature*, 562(7726), pp. 203–209. Available at: https://doi.org/10.1038/s41586-018-0579-z.

517 Chang, J.T. (2020) 'Pathophysiology of Inflammatory Bowel Diseases', *New England Journal*
518 *of Medicine*, 383(27), pp. 2652–2664. Available at: https://doi.org/10.1056/NEJMra2002697.

519 Christ, A., Lauterbach, M. and Latz, E. (2019) 'Western Diet and the Immune System: An
520 Inflammatory Connection', *Immunity*, 51(5), pp. 794–811. Available at:
521 https://doi.org/10.1016/j.immuni.2019.09.020.

522 Coulthard, M.G. *et al.* (2012) 'Eph/Ephrin Signaling in Injury and Inflammation', *The*
523 *American Journal of Pathology*, 181(5), pp. 1493–1503. Available at:
524 https://doi.org/10.1016/j.ajpath.2012.06.043.

525 Czarnewski, P. *et al.* (2019) 'Conserved transcriptomic profile between mouse and human
526 colitis allows unsupervised patient stratification', *Nature Communications*, 10(1), p. 2892.
527 Available at: https://doi.org/10.1038/s41467-019-10769-x.

528 Das, S. *et al.* (2016) 'Mice deficient in Muc4 are resistant to experimental colitis and colitis-
529 associated colorectal cancer', *Oncogene*, 35(20), pp. 2645–2654. Available at:
530 https://doi.org/10.1038/onc.2015.327.

531 Doherty, G. *et al.* (2018) 'European Crohn's and Colitis Organisation Topical Review on
532 Treatment Withdrawal ["Exit Strategies"] in Inflammatory Bowel Disease', *Journal of*
533 *Crohn's and Colitis*, 12(1), pp. 17–31. Available at: https://doi.org/10.1093/ecco-jcc/jjx101.

534 Duan, Y. *et al.* (2018) 'Inflammatory Links Between High Fat Diets and Diseases', *Frontiers*
535 *in Immunology*, 9. Available at:
536 https://www.frontiersin.org/articles/10.3389/fimmu.2018.02649 (Accessed: 19 January 2023).

537 Enriquez, J.R. *et al.* (2022) 'A dietary change to a high-fat diet initiates a rapid adaptation of
538 the intestine', *Cell Reports*, 41(7). Available at: https://doi.org/10.1016/j.celrep.2022.111641.

539 Feagan, B.G. *et al.* (2013) 'Vedolizumab as Induction and Maintenance Therapy for Ulcerative
540 Colitis', *New England Journal of Medicine*, 369(8), pp. 699–710. Available at:
541 https://doi.org/10.1056/NEJMoa1215734.

542 Franke, A. *et al.* (2008) 'Sequence variants in IL10, ARPC2 and multiple other loci contribute
543 to ulcerative colitis susceptibility', *Nature Genetics*, 40(11), pp. 1319–1323. Available at:
544 https://doi.org/10.1038/ng.221.

545 Freeman, K. *et al.* (2021) 'The incidence and prevalence of inflammatory bowel disease in UK
546 primary care: a retrospective cohort study of the IQVIA Medical Research Database', *BMC*
547 *Gastroenterology*, 21(1), p. 139. Available at: https://doi.org/10.1186/s12876-021-01716-6.

548 Fujiyama, Y. *et al.* (2007) 'Butter feeding enhances TNF-α production from macrophages and
549 lymphocyte adherence in murine small intestinal microvessels', *Journal of Gastroenterology*
550 *and Hepatology*, 22(11), pp. 1838–1845. Available at: https://doi.org/10.1111/j.1440-
551 1746.2007.04905.x.

552 Gao, X.-P. *et al.* (2021) 'Integrative Analysis of MUC4 to Prognosis and Immune Infiltration
553 in Pan-Cancer: Friend or Foe?', *Frontiers in Cell and Developmental Biology*, 9. Available at:
554 https://www.frontiersin.org/articles/10.3389/fcell.2021.695544 (Accessed: 10 February 2023).

555 Graham, D.B. and Xavier, R.J. (2020) 'Pathway paradigms revealed from the genetics of
556 inflammatory bowel disease', *Nature*, 578(7796), pp. 527–539. Available at:
557 https://doi.org/10.1038/s41586-020-2025-2.

558 Grandi, A. *et al.* (2019) 'Targeting the Eph/Ephrin System as Anti-Inflammatory Strategy in
559 IBD', *Frontiers in Pharmacology*, 10, p. 691. Available at:
560 https://doi.org/10.3389/fphar.2019.00691.

561 Guda, K. *et al.* (2015) 'Novel recurrently mutated genes in African American colon cancers',
562 *Proceedings of the National Academy of Sciences*, 112(4), pp. 1149–1154. Available at:
563 https://doi.org/10.1073/pnas.1417064112.

564 Halldorsson, B.V. *et al.* (2022) 'The sequences of 150,119 genomes in the UK Biobank',
565 *Nature*, 607(7920), pp. 732–740. Available at: https://doi.org/10.1038/s41586-022-04965-x.

566 Harbord, M. *et al.* (2017) 'Third European Evidence-based Consensus on Diagnosis and
567 Management of Ulcerative Colitis. Part 2: Current Management', *Journal of Crohn's and*
568 *Colitis*, 11(7), pp. 769–784. Available at: https://doi.org/10.1093/ecco-jcc/jjx009.

569 Hasegawa, Y. *et al.* (2020) 'Long-term effects of western diet consumption in male and female
570 mice', *Scientific Reports*, 10(1), p. 14686. Available at: https://doi.org/10.1038/s41598-020-
571 71592-9.

572 Hou, J.K., Abraham, B. and El-Serag, H. (2011) 'Dietary Intake and Risk of Developing
573 Inflammatory Bowel Disease: A Systematic Review of the Literature', *Official journal of the*
574 *American College of Gastroenterology | ACG*, 106(4), p. 563. Available at:
575 https://doi.org/10.1038/ajg.2011.44.

576 Huang, H. *et al.* (2017) 'Fine-mapping inflammatory bowel disease loci to single-variant
577 resolution', *Nature*, 547(7662), pp. 173–178. Available at:
578 https://doi.org/10.1038/nature22969.

579 Ito, R. *et al.* (2006) 'Interferon-gamma is causatively involved in experimental inflammatory
580 bowel disease in mice', *Clinical and Experimental Immunology*, 146(2), pp. 330–338.
581 Available at: https://doi.org/10.1111/j.1365-2249.2006.03214.x.

582 Jha, P., McDevitt, M.T., Halilbasic, E., *et al.* (2018) 'Genetic Regulation of Plasma Lipid
583 Species and Their Association with Metabolic Phenotypes', *Cell Systems*, 6(6), pp. 709-721.e6.
584 Available at: https://doi.org/10.1016/j.cels.2018.05.009.

585 Jha, P., McDevitt, M.T., Gupta, R., *et al.* (2018) 'Systems Analyses Reveal Physiological Roles
586 and Genetic Regulators of Liver Lipid Species', *Cell Systems*, 6(6), pp. 722-733.e6. Available
587 at: https://doi.org/10.1016/j.cels.2018.05.016.

588 Keubler, L.M. *et al.* (2015) 'A Multihit Model: Colitis Lessons from the Interleukin-10–
589 deficient Mouse', *Inflammatory Bowel Diseases*, 21(8), pp. 1967–1975. Available at:
590 https://doi.org/10.1097/MIB.0000000000000468.

591 Khor, B., Gardet, A. and Xavier, R.J. (2011) 'Genetics and pathogenesis of inflammatory
592 bowel disease', *Nature*, 474(7351), pp. 307–317. Available at:
593 https://doi.org/10.1038/nature10209.

Kim, E.R. and Chang, D.K. (2014) ‘Colorectal cancer in inflammatory bowel disease: The risk, pathogenesis, prevention and diagnosis’, *World Journal of Gastroenterology*, 20(29), pp. 9872–9881. Available at: https://doi.org/10.3748/wjg.v20.i29.9872.

Kong, L. *et al.* (2023) ‘The landscape of immune dysregulation in Crohn’s disease revealed through single-cell transcriptomic profiling in the ileum and colon’, *Immunity*, 0(0). Available at: https://doi.org/10.1016/j.immuni.2023.01.002.

Kreuter, R. *et al.* (2019) ‘The role of obesity in inflammatory bowel disease’, *Biochimica et Biophysica Acta (BBA) - Molecular Basis of Disease*, 1865(1), pp. 63–72. Available at: https://doi.org/10.1016/j.bbadis.2018.10.020.

Kulakovskiy, I.V. *et al.* (2018) ‘HOCOMOCO: towards a complete collection of transcription factor binding models for human and mouse via large-scale ChIP-Seq analysis’, *Nucleic Acids Research*, 46(Database issue), pp. D252–D259. Available at: https://doi.org/10.1093/nar/gkx1106.

Langfelder, P. and Horvath, S. (2008) ‘WGCNA: an R package for weighted correlation network analysis’, *BMC Bioinformatics*, 9(1), p. 559. Available at: https://doi.org/10.1186/1471-2105-9-559.

Li, H. *et al.* (2019) ‘Identifying gene function and module connections by the integration of multispecies expression compendia’, *Genome Research* [Preprint]. Available at: https://doi.org/10.1101/gr.251983.119.

Li, H. *et al.* (2022) ‘Integrative systems analysis identifies genetic and dietary modulators of bile acid homeostasis’, *Cell Metabolism*, 34(10), pp. 1594-1610.e4. Available at: https://doi.org/10.1016/j.cmet.2022.08.015.

Li, H. and Auwerx, J. (2020) ‘Mouse Systems Genetics as a Prelude to Precision Medicine’, *Trends in genetics: TIG*, 36(4), pp. 259–272. Available at: https://doi.org/10.1016/j.tig.2020.01.004.

Li, J.-Y. *et al.* (2021) ‘IRF/Type I IFN signaling serves as a valuable therapeutic target in the pathogenesis of inflammatory bowel disease’, *International Immunopharmacology*, 92, p. 107350. Available at: https://doi.org/10.1016/j.intimp.2020.107350.

622 Liberzon, A. *et al.* (2011) 'Molecular signatures database (MSigDB) 3.0', *Bioinformatics*,
623 27(12), pp. 1739–1740. Available at: https://doi.org/10.1093/bioinformatics/btr260.

624 Liu, Z. *et al.* (2000) 'IL-15 is highly expressed in inflammatory bowel disease and regulates
625 local T cell-dependent cytokine production', *Journal of Immunology (Baltimore, Md.: 1950)*,
626 164(7), pp. 3608–3615. Available at: https://doi.org/10.4049/jimmunol.164.7.3608.

627 Lutsey, P.L., Steffen, L.M. and Stevens, J. (2008) 'Dietary Intake and the Development of the
628 Metabolic Syndrome', *Circulation*, 117(6), pp. 754–761. Available at:
629 https://doi.org/10.1161/CIRCULATIONAHA.107.716159.

630 Maconi, G. *et al.* (2010) 'Pre-illness changes in dietary habits and diet as a risk factor for
631 inflammatory bowel disease: A case-control study', *World Journal of Gastroenterology*,
632 16(34), pp. 4297–4304. Available at: https://doi.org/10.3748/wjg.v16.i34.4297.

633 Mähler, M. *et al.* (1998) 'Differential susceptibility of inbred mouse strains to dextran sulfate
634 sodium-induced colitis', *American Journal of Physiology-Gastrointestinal and Liver*
635 *Physiology*, 274(3), pp. G544–G551. Available at:
636 https://doi.org/10.1152/ajpgi.1998.274.3.G544.

637 Maurya, S.K. *et al.* (2023) 'Western Diet Causes Heart Failure With Reduced Ejection Fraction
638 and Metabolic Shifts After Diastolic Dysfunction and Novel Cardiac Lipid Derangements',
639 *JACC: Basic to Translational Science*, 0(0). Available at:
640 https://doi.org/10.1016/j.jacbts.2022.10.009.

641 McGuckin, M.A. *et al.* (2011) 'Mucin dynamics and enteric pathogens', *Nature Reviews*
642 *Microbiology*, 9(4), pp. 265–278. Available at: https://doi.org/10.1038/nrmicro2538.

643 Misiorek, J.O. *et al.* (2016) 'Keratin 8-deletion induced colitis predisposes to murine colorectal
644 cancer enforced by the inflammasome and IL-22 pathway', *Carcinogenesis*, 37(8), pp. 777–
645 786. Available at: https://doi.org/10.1093/carcin/bgw063.

646 Mogensen, T.H. (2019) 'IRF and STAT Transcription Factors - From Basic Biology to Roles
647 in Infection, Protective Immunity, and Primary Immunodeficiencies', *Frontiers in Immunology*,
648 9. Available at: https://www.frontiersin.org/articles/10.3389/fimmu.2018.03047 (Accessed: 19
649 January 2023).

650 Molodecky, N.A. *et al.* (2011) 'Challenges associated with identifying the environmental
651 determinants of the inflammatory bowel diseases', *Inflammatory Bowel Diseases*, 17(8), pp.
652 1792–1799. Available at: https://doi.org/10.1002/ibd.21511.

653 Mottis, A. *et al.* (2022) 'Tetracycline-induced mitohormesis mediates disease tolerance against
654 influenza', *The Journal of Clinical Investigation*, 132(17). Available at:
655 https://doi.org/10.1172/JCI151540.

656 Mun, J., Hur, W. and Ku, N.-O. (2022) 'Roles of Keratins in Intestine', *International Journal*
657 *of Molecular Sciences*, 23(14), p. 8051. Available at: https://doi.org/10.3390/ijms23148051.

658 Nadeau, J.H. and Auwerx, J. (2019) 'The virtuous cycle of human genetics and mouse models
659 in drug discovery', *Nature Reviews. Drug Discovery*, 18(4), pp. 255–272. Available at:
660 https://doi.org/10.1038/s41573-018-0009-9.

661 Nayak, R.R. *et al.* (2009) 'Coexpression network based on natural variation in human gene
662 expression reveals gene interactions and functions', *Genome Research*, 19(11), pp. 1953–1962.
663 Available at: https://doi.org/10.1101/gr.097600.109.

664 Peters, L.A. *et al.* (2017) 'A functional genomics predictive network model identifies
665 regulators of inflammatory bowel disease', *Nature Genetics*, 49(10), pp. 1437–1449. Available
666 at: https://doi.org/10.1038/ng.3947.

667 Porcu, E. *et al.* (2021) 'Differentially expressed genes reflect disease-induced rather than
668 disease-causing changes in the transcriptome', *Nature Communications*, 12(1), p. 5647.
669 Available at: https://doi.org/10.1038/s41467-021-25805-y.

670 Ritchie, M.E. *et al.* (2015) 'limma powers differential expression analyses for RNA-
671 sequencing and microarray studies', *Nucleic Acids Research*, 43(7), p. e47. Available at:
672 https://doi.org/10.1093/nar/gkv007.

673 Rutgeerts, P. *et al.* (2005) 'Infliximab for Induction and Maintenance Therapy for Ulcerative
674 Colitis', *New England Journal of Medicine*, 353(23), pp. 2462–2476. Available at:
675 https://doi.org/10.1056/NEJMoa050516.

Serino, M. *et al.* (2012) 'Metabolic adaptation to a high-fat diet is associated with a change in the gut microbiota', *Gut*, 61(4), pp. 543–553. Available at: https://doi.org/10.1136/gutjnl-2011-301012.

Shah, S.C. and Itzkowitz, S.H. (2022) 'Colorectal Cancer in Inflammatory Bowel Disease: Mechanisms and Management', *Gastroenterology*, 162(3), pp. 715-730.e3. Available at: https://doi.org/10.1053/j.gastro.2021.10.035.

Stolzer, I. *et al.* (2021) 'An IFN-STAT Axis Augments Tissue Damage and Inflammation in a Mouse Model of Crohn's Disease', *Frontiers in Medicine*, 8. Available at: https://www.frontiersin.org/articles/10.3389/fmed.2021.644244 (Accessed: 12 January 2023).

Tannock, L.R. *et al.* (2018) 'Serum amyloid A3 is a high density lipoprotein-associated acute-phase protein', *Journal of Lipid Research*, 59(2), pp. 339–347. Available at: https://doi.org/10.1194/jlr.M080887.

Tilg, H. *et al.* (2002) 'Treatment of Crohn's disease with recombinant human interleukin 10 induces the proinflammatory cytokine interferon γ', *Gut*, 50(2), pp. 191–195. Available at: https://doi.org/10.1136/gut.50.2.191.

Uhlén, M. *et al.* (2015) 'Tissue-based map of the human proteome', *Science*, 347(6220), p. 1260419. Available at: https://doi.org/10.1126/science.1260419.

Williams, E.G. *et al.* (2016) 'Systems proteomics of liver mitochondria function', *Science*, 352(6291). Available at: https://doi.org/10.1126/science.aad0189.

Wu, Y. *et al.* (2014) 'Multilayered genetic and omics dissection of mitochondrial activity in a mouse reference population', *Cell*, 158(6), pp. 1415–1430. Available at: https://doi.org/10.1016/j.cell.2014.07.039.

Yang, X. *et al.* (1999) 'Targeted disruption of SMAD3 results in impaired mucosal immunity and diminished T cell responsiveness to TGF-β', *The EMBO Journal*, 18(5), pp. 1280–1291. Available at: https://doi.org/10.1093/emboj/18.5.1280.

Ye, R.D. and Sun, L. (2015) 'Emerging functions of serum amyloid A in inflammation', *Journal of Leukocyte Biology*, 98(6), pp. 923–929. Available at: https://doi.org/10.1189/jlb.3VMR0315-080R.

704 Yoshihara, K. *et al.* (2006) 'Role of interleukin 15 in colitis induced by dextran sulphate
705 sodium in mice', *Gut*, 55(3), pp. 334–341. Available at:
706 https://doi.org/10.1136/gut.2005.076000.

707 Yu, G. *et al.* (2012) 'clusterProfiler: an R Package for Comparing Biological Themes Among
708 Gene Clusters', *OMICS: A Journal of Integrative Biology*, 16(5), pp. 284–287. Available at:
709 https://doi.org/10.1089/omi.2011.0118.

710 Zeevi, D. *et al.* (2015) 'Personalized Nutrition by Prediction of Glycemic Responses', *Cell*,
711 163(5), pp. 1079–1094. Available at: https://doi.org/10.1016/j.cell.2015.11.001.

712 Zhao, D. *et al.* (2020) 'High-Fat Diet Promotes DSS-Induced Ulcerative Colitis by
713 Downregulated FXR Expression through the TGFB Pathway', *BioMed Research International*,
714 2020, p. e3516128. Available at: https://doi.org/10.1155/2020/3516128.

715
716

Figure Legends

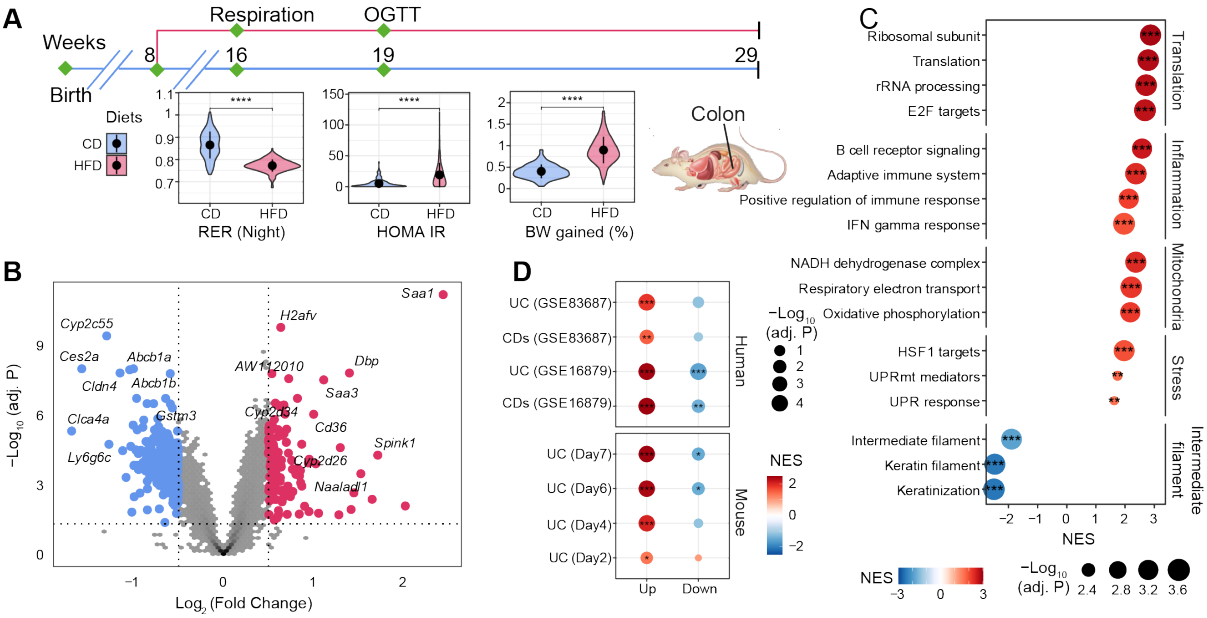

Figure 1. The effect of long-term HFD on gene expression in BXD colons. (**A**) Graphical representation of a pipeline of a previously described BXD mouse study (Williams *et al.*, 2016). Mice were fed HFD or CD starting from 8 weeks of age and metabolic phenotyping was performed as indicated. Mice were sacrificed at 29 weeks of age and multiple organs were collected and frozen for further analyses. BXD colon transcriptomes were analyzed in this study. CD: chow diet indicated in blue, HFD: high-fat diet indicated in red. P values were calculated by two-tailed Student's t-test and indicated as follows: * P <0.05; ** P <0.01; *** P <0.001; **** P <0.0001. (**B**) Volcano plot showing the HFD effect on BXD colon transcriptomes compared to CD and the up- and down-regulated differentially expressed genes (DEGs, absolute Log_2(Fold Change) > 0.5 and BH-adjusted P value (adj. P) < 0.05) were highlighted in red and blue, respectively. (**C**) Gene set enrichment analysis showing the effect of HFD on gene expression in BXD colons. Gene sets were grouped into five categories: Translation, Inflammation, Mitochondria, Stress, and Intermediate filament. Normalized enrichment scores (NES) were represented by color and -Log_{10} (BH-adj. P) were represented by dot size and indicated as follows: * Adjusted P value <0.05; ** Adjusted P value <0.01; *** Adjusted P value <0.001. (**D**) Enrichment analysis of molecular signatures of mouse and human IBD on the transcriptome of BXD colons. UC: Ulcerative colitis, CDs: Crohn's disease

The following figure supplement is available for figure 1:

Figure supplement 1. Transcriptome profile in BXD colons.

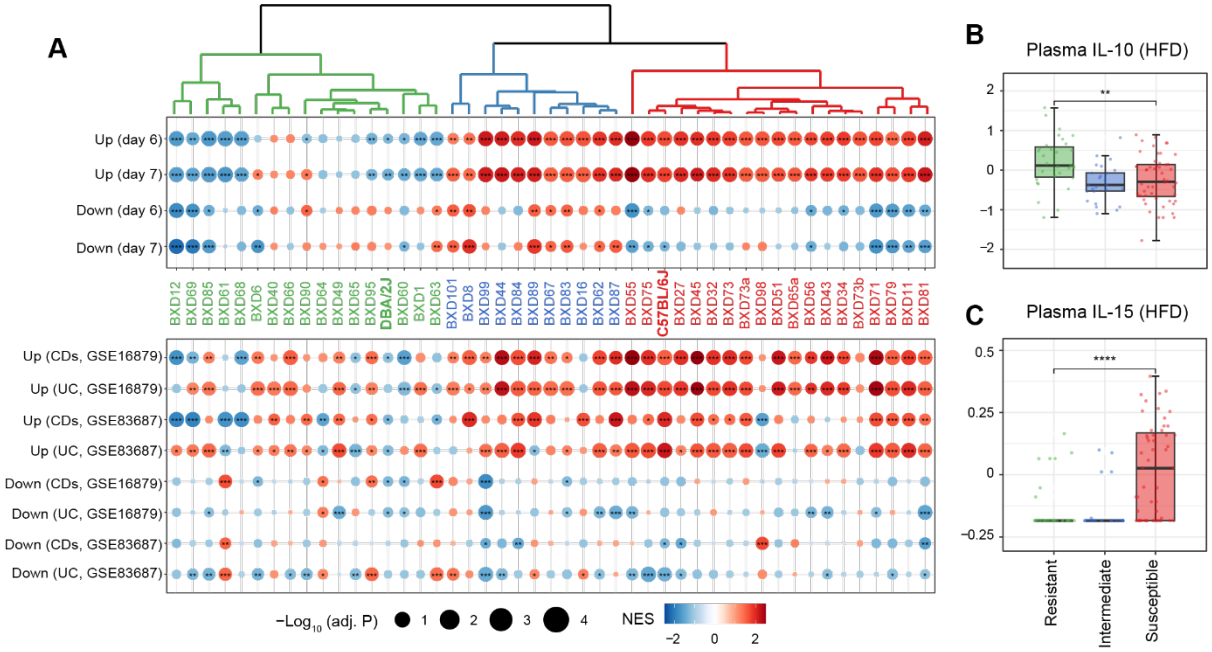

739

740 **Figure 2. Identifying susceptible strains to HFD-induced IBD-like inflammation and their**
741 **effect on plasma cytokines.** (**A**) Enrichment analysis of the molecular signatures in human
742 (**bottom panel**) and mouse IBD (**top panel**) models on the gene expression of individual BXD
743 colons. Dendrogram showing the propensity to develop a mouse IBD-like signature among
744 BXD strains upon HFD. BXD strains were divided into three clusters: susceptible (in red),
745 intermediate (in blue), and resistant strains (in green). Normalized enrichment scores (NES)
746 were represented by color and -Log_{10}(BH-adjusted P values) were represented by dot size and
747 indicated as follows: * Adjusted P value <0.05; ** Adjusted P value <0.01; *** Adjusted P
748 value <0.001. UC: Ulcerative colitis, CDs: Crohn's disease (**B, C**) Boxplots showing the effect
749 of susceptible strains on plasma IL-10 (**B**) and IL-15 (**C**) level compared to resistant strains. P
750 values were calculated by two-tailed Student's t-test and indicated as follows: * P <0.05; ** P
751 <0.01; *** P <0.001; **** P <0.0001.
752

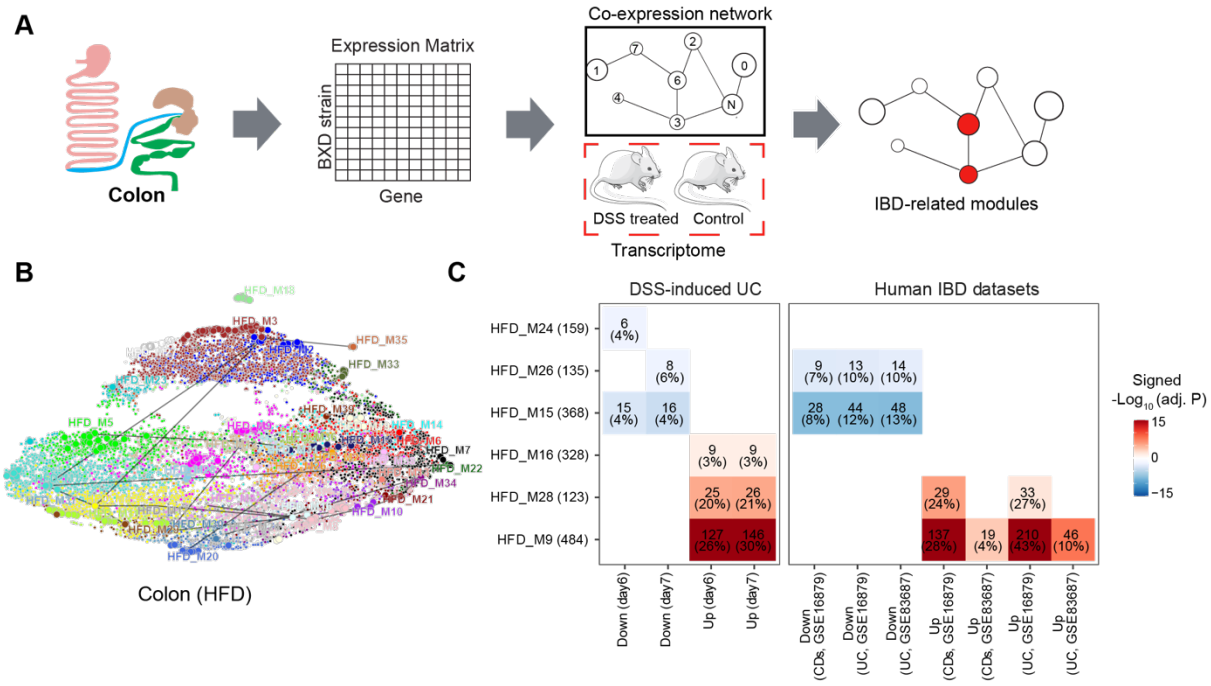

Figure 3. Identifying IBD-related gene modules. (**A**) Pipeline for exploring the IBD-associated gene modules. A co-expression gene network was constructed based on the transcriptome of BXD colons under HFD. IBD-associated modules were then defined as gene modules under HFD that are significantly clustered in mouse DSS-induced UC signatures. (**B**) UMAP representation of the co-expression gene network under HFD. 39 co-expression modules are represented in the corresponding color and the correlated modules (Spearman correlation coefficient between the eigengene of modules > 0.7) were linked by a grey line. (**C**) Heatmap showing the enrichment of co-expression modules in mouse and human IBD gene signatures and the number and percentage of enriched genes were labeled. The number of enriched genes divided by the number of genes involved in the respective module was defined as the percentage of enriched genes. Signed $-Log_{10}$(adj. P) indicated BH-adjusted P value and the enriched gene set. Enriched modules of up- and down-regulated genes upon disease were highlighted in red and blue, respectively. UC: Ulcerative colitis, CDs: Crohn's disease.

The following figure supplement is available for figure 3:

Figure supplement 1. Exploring IBD-associated co-expression modules under CD.

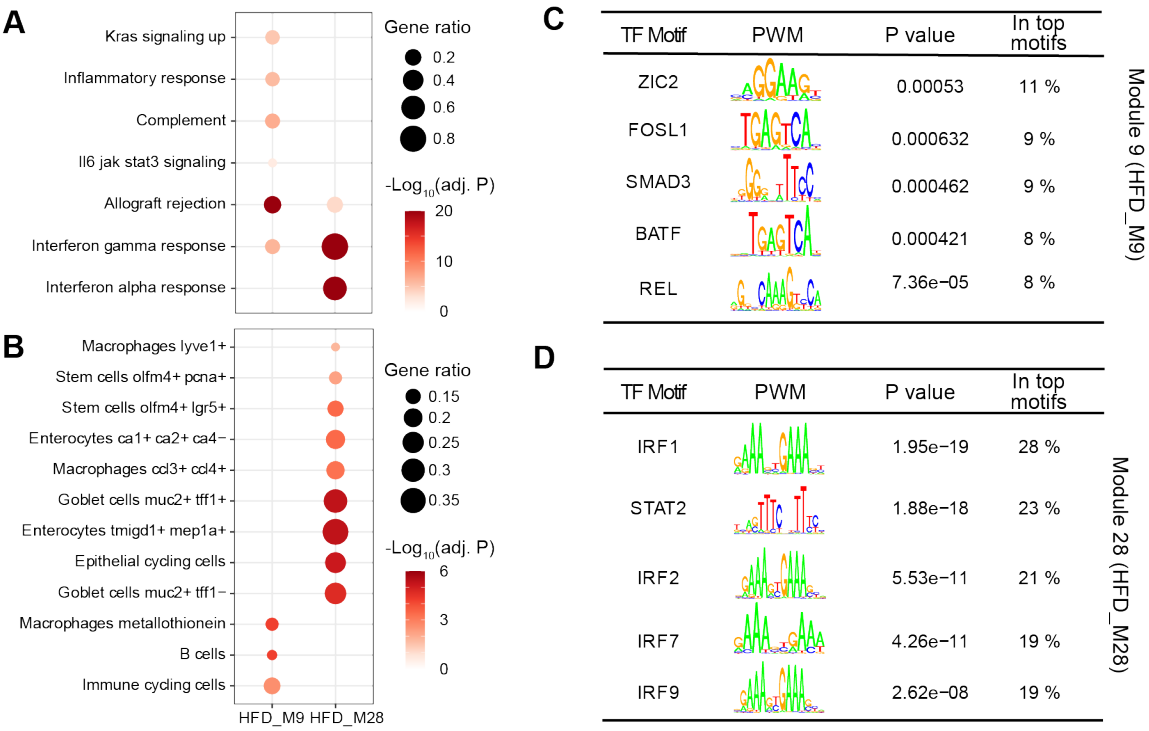

TF Motif	PWM	P value	In top motifs
ZIC2		0.00053	11 %
FOSL1		0.000632	9 %
SMAD3		0.000462	9 %
BATF		0.000421	8 %
REL		7.36e−05	8 %

TF Motif	PWM	P value	In top motifs
IRF1		1.95e−19	28 %
STAT2		1.88e−18	23 %
IRF2		5.53e−11	21 %
IRF7		4.26e−11	19 %
IRF9		2.62e−08	19 %

Figure 4. Biological interrogation of identified IBD-related modules. (**A**, **B**) Dot plots showing the enrichment of IBD-related modules in hallmark genesets (**A**) and cell-type gene signatures of inflamed colon in Crohn's disease patients (**B**). Gene ratios higher than 0.1 are shown and represented by dot size. Dots are colored by -$\log_{10}$(BH-adjusted P values). (**C**, **D**) The enriched motifs for promoters of the genes involved in module HFD_M9 (**C**) and HFD_M28 (**D**). The significantly enriched motifs (P value < 0.001) were ranked based on the percentage of enriched promoters (In top motifs) and then the top five TFs were selected. TF: Transcription factor. PWM: Positional weight matrix.

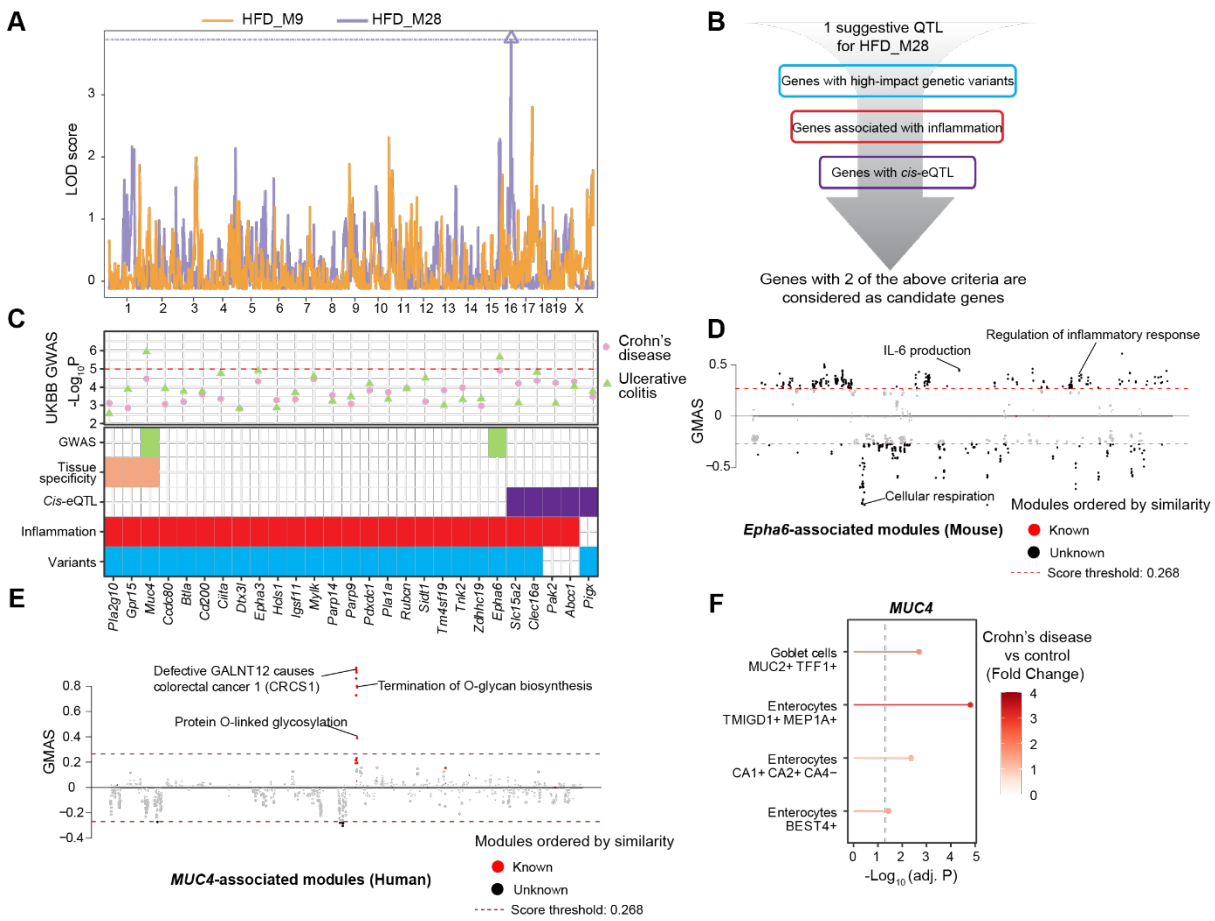

Figure 5. ModQTL mapping for two IBD-related modules and the prioritization of candidate genes. (**A**) Manhattan plot showing the ModQTL mapping result for disease-related modules HFD_M9 and HFD_M28. ModQTL maps of HFD_M9 and HFD_M28 are indicated in orange and purple, respectively. The threshold calculated by permutation test ($P < 0.1$) for HFD_M28 is represented by a purple dashed line. (**B**) The filtering criteria for selecting candidate genes under the ModQTL peak for HFD_M28. Genes with 2 of the described criteria are considered as candidate genes. (**C**) The most significant associations between 27 candidate genes under the ModQTL peak and Crohn's disease or UC identified through GWAS according to whole genome sequence in the human UKBB are shown in the scatter plot (**top panel**). Crohn's disease and UC are indicated by pink circle and green triangle, respectively. The threshold ($-Log_{10}P$ value = 5) is represented by a red dashed line. Heatmap showing the identified 27 candidate genes of module HFD_M28 (**bottom panel**). Variants colored in blue indicate genes with high-impact genetic variants in BXD mice (including missense, frameshift, initiator codon, splice donor, splice acceptor, in-frame deletion, in-frame insertion, stop lost, stop gained). Inflammation is indicated in red and represents genes associated with inflammation based on literature mining. *Cis*-eQTL colored in purple indicates genes with *Cis*-

eQTLs. Tissue specificity colored in orange means genes that are highly expressed in human intestine (data were downloaded from human protein atlas, https://www.proteinatlas.org/humanproteome/tissue/intestine (Uhlén *et al.*, 2015)). GWAS result of UC in UKBB colored in green indicates that genes are significantly associated with human UC. (**D**, **E**) Manhattan plots showing the associated gene expression modules of *Epha6* in mouse gastro-intestinal tract (**D**) and that of *MUC4* in human gastro-intestinal tract (**E**) (data from https://systems-genetics.org/gmad (Li *et al.*, 2019)). The threshold is represented by the red dashed line (absolute Gene-Module Association Score (GMAS) >= 0.268). Terms above the threshold are identified as the significant associated terms. GO terms or gene modules are ranked by similarity. Known associated terms are shown as red dots and new significant associated terms are colored in black. (**F**) Dot plot showing that the expression of *MUC4* was higher in four cell types of human inflamed colon with Crohn's disease.

The following figure supplement is available for figure 5:

Figure supplement 1. Genome-wide association studies (GWAS) for Ulcerative colitis (UC) and Crohn's disease (CDs) in humans.

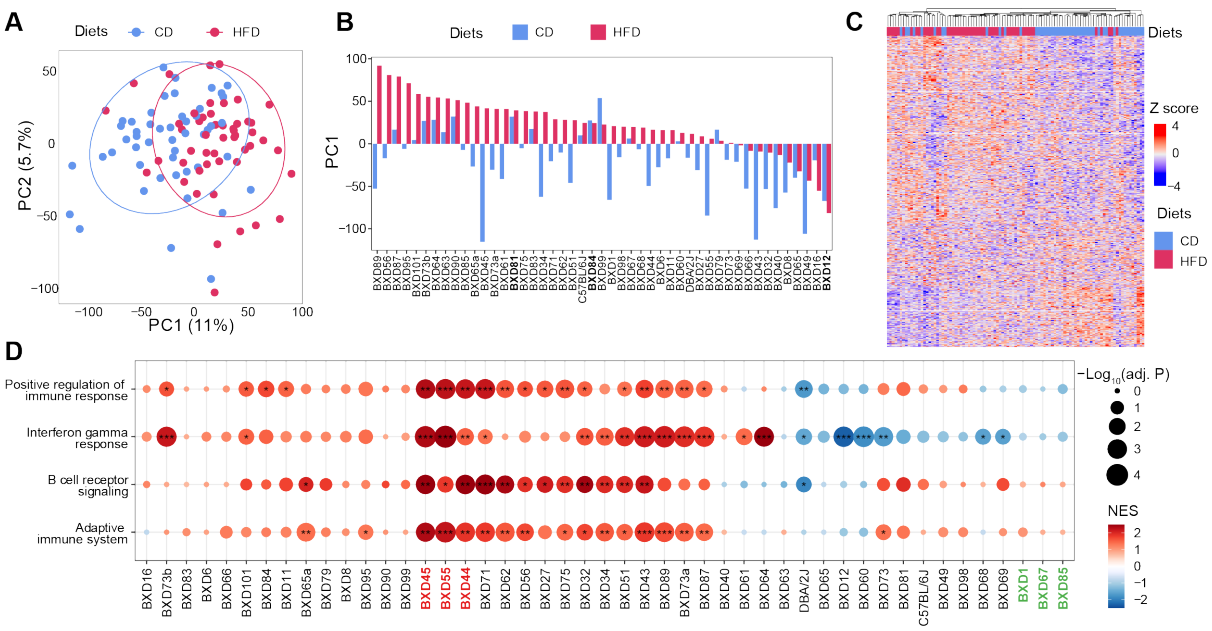

Figure 1—figure supplement 1. Transcriptome profile in BXD colons. (**A**) Principal-component analysis (PCA) of the microarray profiles of BXD colons under high-fat (HFD, indicated in red) or chow diet (CD, represented in blue). (**B**) Bar plot showing the primary principle (PC1) calculated by PCA of the colon transcriptomes in each BXD strain fed with CD (blue) or HFD (red). BXD strains highlighted in bold mean they are more resistant to dietary challenges. (**C**) Heatmap showing unsupervised hierarchical clustering of colon transcriptome in both the CD and HFD fed BXDs. (**D**) Enrichment analysis of inflammation-related genesets showing the effect of HFD on gene expression in individual BXD colon. Normalized enrichment scores (NES) were represented by color and -Log_{10}(BH-adjusted P values) were represented by dot size and indicated as follows: * Adjusted P value < 0.05; ** Adjusted P value < 0.01; *** Adjusted P value < 0.001. BXD strains highlighted in red represent the 3 most susceptible strains to gut inflammation upon HFD. BXD strains colored in green show no significant enrichment in gut inflammation.

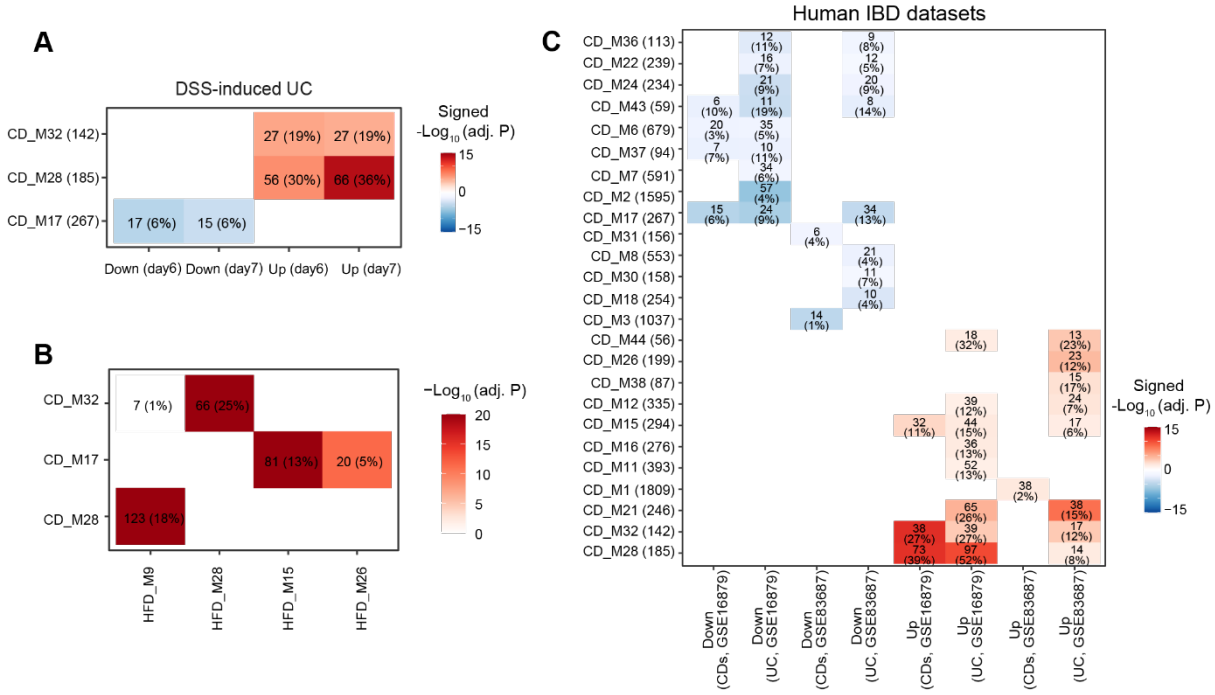

Figure 3—figure supplement 1. Exploring IBD-associated co-expression modules under CD. (**A**) Heatmap showing modules enriched in mouse IBD gene signatures and the number and percentage of enriched genes were labeled. The number of enriched genes divided by the number of genes involved in the respective module was defined as the percentage of enriched genes. Signed $-Log_{10}$(adj. P) indicated BH-adjusted P value and the enriched gene set. Enriched modules of up- and down-regulated genes upon disease were highlighted in red and blue, respectively. (**B**) Heatmap showing the similarity of co-expression modules identified under CD or HFD. The number and percentage of overlapped genes were labeled. The number of overlapped genes divided by the number of genes involved in the respective module in HFD was defined as the percentage of overlapped genes. Adjusted P values calculated by BH were indicated by color. (**C**) Heatmap showing the modules under CD enriched in human IBD gene signatures and the number and percentage of enriched genes were labeled. UC: Ulcerative colitis, CDs: Crohn's disease.

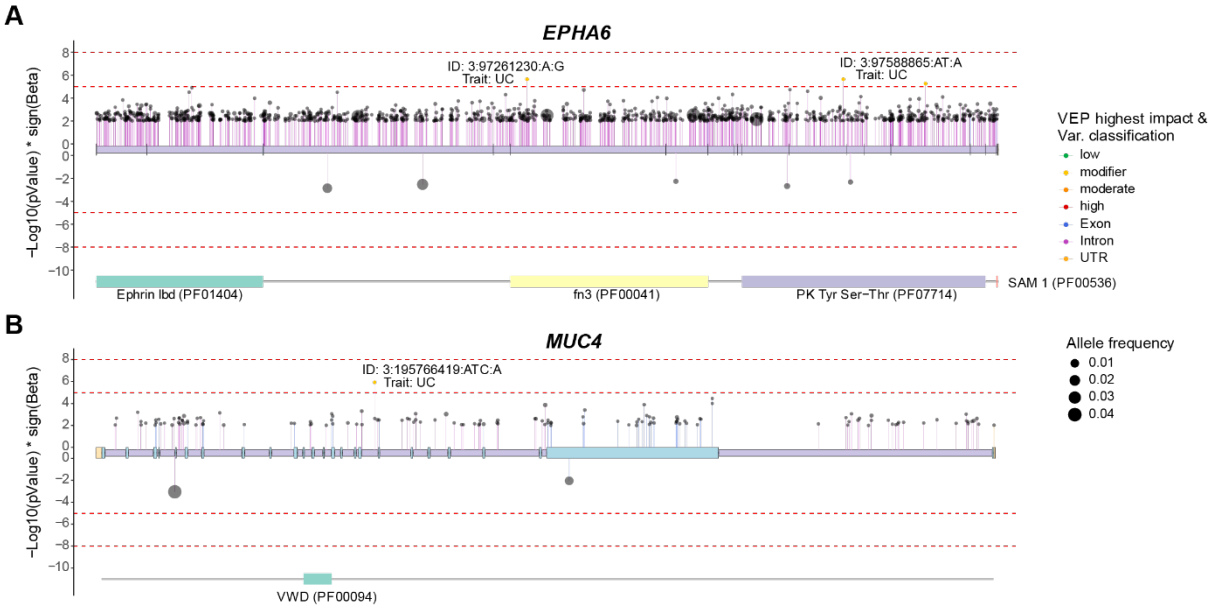

845

846 **Figure 5—figure supplement 1. Genome-wide association studies (GWAS) for Ulcerative**
847 **colitis (UC) and Crohn's disease (CDs) in humans.** (**A**, **B**) Lollipop plots showing UC- or
848 CDs-associated genetic variants of *EPHA6* (**A**) and *MUC4* (**B**) based on UKBB whole genome
849 sequence data. Variants effect were predicted and their classification are represented by color.
850 VEP: Variant Effect Prediction.

851

852 **Tables**

853 Table 1: Gene signatures of mouse and human IBDs

Disease	Source	DEGs	Thresholds	Species	Tissues
DSS-induced UC	GSE131032 (Czarnewski *et al.*, 2019)	Author-provided DEGs	absolute log2FC >1 & BH-adjusted P value < 0.05	Mouse	Colon
Crohn's disease & UC	GSE16879 (Arijs *et al.*, 2009; Li *et al.*, 2019)	Author-provided DEGs	absolute FC >1 & BH-adjusted P value <0.01	Human	Colon
Crohn's disease & UC	GSE83687 (Peters *et al.*, 2017)	DEGs computed by limma package (Ritchie et al., 2015)	absolute log2FC >1 & BH-adjusted P value <0.001	Human	Colon
Crohn's disease	SCP1884 (Kong *et al.*, 2023)	Author-provided DEGs	DE coefficient >1 & BH-adjusted P value <0.05	Human	Colon

854

855

856 **Table Supplements and Legends**

857 **Appendix 1 - Table 1. Co-expression networks under CD or HFD. Related to Figure 3**

858 **Appendix 1 - Table 2. Genes under QTL peak of module HFD_M28. Related to Figure 5**

859 **Appendix 1 - Table 3. G-MAD result for *Epha6* in mice and *MUC4* in humans. Related to**

860 **Figure 5.**

861 **Appendix 1 - Table 4. Medicine for human IBD.**

862

863